Brief History of Switched Reluctance Motor

[1.]Deepa Bajpai [2.]Dr. Vivek Kant Jogi,

P.Hd Scholer, Department of Electrical Engineering, MSEIT, Raipur-492004(C.G.)
Asst. Prof. Department MSEIT, Raipur-492004(C.G.)
Corresponding Author: Deepa Bajpai

***Abstract** – The generated torque ripple and acoustic noise in switched reluctance motors (SRM) can be considered as one of the major disadvantages of the motor. It is mainly due to frequent switching of phases for rotation of the motor and changes of the air gap length between the rotor and stator teeth. It decreases the average developed torque, diminish the efficiency, causes noise and vibration in the motor. So, in order to improve the performance of SRM and extend its applications in industry, it is essential to reduce these torque ripple. So far, many torque ripple reduction methods have been introduced. These have been done through changing and improving the structure and geometry of the motor or using some control strategies. This paper reviews a variety of control strategies to reduce the torque ripple in SRM. Each of the methods described in details. Different techniques are compared and the best and most efficient one is introduced.*
***Keywords:** switched reluctance motors, torque ripple reduction*

I. Introduction

The concept of SR motor can be traced back to 1838, of the locomotive era [2]. The early attempts faced serious limitations on account of inadequate switches and poor electromagnetic and mechanical design. However, in 1980 the foundation for the SR motor and its practical design may be reckoned with Prof. Lawrenson's paper [1]. At the first instance, in 1979 Ray and Davis [3] identified a simplified linear model, explained the basic principles and developed the important design and performance criteria. The development of non-linear model by Lawrenson [1] confirmed the basic properties of the machine and enabled to predict the performance more accurately and led to the commercial development of SR motor. During 1981-92 Several design methods [4], machine configurations [12, 13, 14], analysis [5-8], converter topologies [9] and control strategies [10, 11, 12] emerged. Till the publication (1989) of Millers' book [1] on 'Brushless Permanent-Magnet and Reluctance Motor Drives', all the concerned materials related to SR motors were scattered in different conference proceedings and various journals. Miller gave a brief introduction of the different aspects of the motor and its controller in his above mentioned book in a textbook form. The second book [12] authored by Miller (1993) explains all the features of SR motor drive in more detail. This book depicts the qualitative aspects of SR motor in a very judicious manner without exaggerating the facts. Besides the potential of SR motor drives, the limitations are also well covered and that gives a good insight to a researcher about the state-of-the-art of this motor. After the publication of Miller's book, a lot more work has been done on the various aspects of SR motor, like design, modelling, control, position/shaft sensorless operations, torque ripple minimization, acoustic noise reduction etc.

To avoid stepwise current or flux linkage commands, several schemes were also proposed in [15] - [20]. Husain(1997) *et al.* [17] and Ilic-Spong (1987) *et al.* [16] proposed a sinusoidal function and an exponential function as a torque distribution function, respectively . The basic idea was to distribute the desired torque to two adjacent phases during predetermined commutation interval using the torque distribution function. By assuming an ideal inductance profile, however, incorrect current commands caused torque error and by choosing a short commutation interval the rates of change of currents or flux linkages could not be much reduced. On the other hand,in 1992 Wallace *et al.* [17] linearly decreased the outgoing phase current and increased the incoming phase current during commutation accepting possible torque error. In 1996 Kim *et al.* [18] proposed a torque distribution function, which could minimize the rates of change of currents over the commutation interval.

In some of these control schemes, ideal inductance profiles were assumed and more importantly all of them didn't consider the effects of the mutual inductance during commutation. J. C. Moreiara et.al. (1989) mentioned the effects of the mutual inductance were in [13] and H. H. Moghbelli et.al. (1988) in [14] but a controller to compensate the effects was not proposed. The possibility of two-phase excitation was introduced by P. Pillay et. all. (1999) shown in [19] but it also only mentioned the effects of mutual coupling without suggesting any active control scheme to overcome the effects. In some applications, the torque ripple caused by

---

the mutual inductance may not be acceptable. Therefore, the effect of mutual coupling should be analyzed to decide whether it is negligible or not.

In addition, J. Faiz,et.all, (2000) had many attempts to decrease the torque ripple using advanced electronics control techniques including optimization of controlling parameters such as supply voltage, commutation angles and current level [24,25]. One of the old methods for torque ripple reduction uses torque/ current/rotor angular angle characteristics to control SRM drive system. In 1991-92 these characteristics can be obtained using theoretical methods by R.C. Kavanagh and D.S. Schramm [26, 27] or by J.C. Moreira had static test [28] and then apply interpolation routine. Some methods try to reduce torque ripple through compensation, deformation and current optimization. In1996 , I. Husain , PWM control technique has been used to improve the current in which the current traces a contour to develop a constant torque [29]. This technique is appropriate over low speeds.

By N.C. Sahoo et all, in 2000-01, Current compensation has been used in [30-32]. To generate current profile, Fuzzy-logic method has been applied in [30] which compensate the non-linearity of the system well. In [31], reference current is modified through adding output of a fuzzy-natural compensator by J.A. Dente . In 2011,by L. Kalaivani et. all, phase current compensation has been implemented by fuzzy-logic controller and ANFIS, which leads to good results up to the base speed [32]. By R. Mitra, Phase current shaping method has been used in [33, 34]. In 2001, by I. Agirm et. all. ,Phase current can be improved by injecting and adjusting proper harmonic terms in the current and cancelling the harmonics [35-37].

An appropriate speed controller design for minimizing the torque ripple and obtaining high performance has been suggested by H. Tahresima in 2011[38]. In [39], controlling sum of square of phase currents plus sliding mode control has been recommended by N. Inanc in 2003. In [40], phase current optimization method in a positive semi-sinusoidal form and its control has been used by N.T. Shaked, in 2005. In 2009 by R. Gobbi et,all.[41], the hysteresis controller has been optimized in order to inject a suitable current to the drive system.

One other method is designing and obtaining particular current [42]. Selection of optimal switching angles based on the maximum torque and current ratio criterion is appropriate for high speed SRM. In this case, the minimum torque ripple criterion can be approximated over low speed range. Attempt has been made in 2003 by C. Mademlis et.all., [43-47] to optimize on- and off-switching angles for reduction of torque ripple in SRM. D.H. Lee in 2009 had introduce the torque distribution function technique may be used to alleviate the torque ripple [48-51]. This technique controls torque variation rate over commutation period according to a pre-defined torque distribution function.

In 2013, in order to take into account a precise non-linear model for inclusion of SRM drive non-linearity, advanced methods such as artificial natural network (ANN), fuzzy-logic or their combination can be applied by J. Faiz [52, 53]. In ANN non-linearity of SRM characteristics is trained by NNs and then current graph for ripple reduction is obtained by . In [54, 55], ANN has been used as an intelligent controller by Y. Cai in 2006-07. The fuzzy-logic model has the advantageous of simple mathematical computations in processing fuzzy-logic rules which leads to a quick operation. Fuzzy-logic has been used as an intelligent method by M. Rodrigues in [56-60].

J. Faiz in 2010, can be also used torque control techniques for torque ripple reduction [61]. A torque controller has been designed K. Russa and I. Husain in 2002 in [62-64] while in [65] the ripple have been reduced by controlling the excited phase output torque through adjusting the relevant co-energy by tracking the co-energy diagram by K.F. Wong in 2009 . Direct torque control (DTC) has been followed in [66, 67]. A new pattern called two-phase excitation has been suggested in [68] by C. Ma 2013, which have the highest average torque and lowest torque ripple compared to the two conventional patterns. The attempt has been made in [69,70] to decrease the torque ripple through changing the geometry of the motor by D.H. Lee in 2013. In [71], a four-level converter has been utilized to improve the torque and speed ripple which also shorten the response time and current peak in SRM by J.W. Ahn in 2007.

One of useful and efficient method in reducing the cost and enhancing efficiency is decreasing the losses and number of switches in each leg of the converter. A. Deriszadeh in 2011, has been introduced a new converter with one switch per phase in [72] which have low cost and high efficiency advantages as well as lower torque ripple. Novel and advanced methods and algorithms have been suggested by E. Daryabeigi et all, in 2014, in [73-76] in order adjust the speed or current controller and reduce the torque ripple.

In [76] D. Suitra et.all. has been proposed a method which is capable of estimating the rotor position models for SRM within acceptable accuracy limits and are sure to present a superior performance when applied to modelling, prediction and control in 2012. The accuracy and ease of rotor position estimation of this model validate that this technique can be applied to the real time control of SR machine and can be effectively utilized for obtaining the subsequent controller design.

R.A. Gupta et all. In 2010 proposed an approach for sensorless rotor position estimation in SRM drive. A novel fuzzy logic based rotor position estimation technique is explained and simulated, which provides an

alternative way of measuring the rotor position in SRM drive in [77]. Maged N.F. Nashed et. all. In 2014 presented the study on determination of a unique of turn-on and turn-off angeles that gives optimum performance of the SRM during no-load starting[78]. At steady state, for constant turn-off angle, if the advance of the turn-on angle increases, then the average source current, the average total torque and the average total torque per ampere are directly proportional to advance of turn-on angle. The motor speed is directly proportional to advance of turn-on angle. And at steady state, for constant turn-on angle; if the retard of the turn-off angle increases (*i.e*, increasing value of θoff), then the average source current, the average total torque and the average total torque per ampere are directly proportional to retard of turn-off angle. The motor speed is directly proportional to retard of turn-off angle.

A torque ripple minimization technique based on indirect dynamic torque control was introduced by Zhen Zhong Ye et all. In 2000. A corresponding control block based on a torque controller and a fuzzy logic controller was described. Simulation results showed the feasibility of the developed approach to minimize the torque ripple, especially in the low-speed region. However, as the SRM operates in the high-speed region, the rate of change of the phase current limits any torque-ripple improvement. On the other hand, extending the phase commutation period to allow for negative torque may be beneficial to minimize the torque ripple. Krzysztof Bieńkowski in 2004 worked out software makes possible to choose set of constructional parameters of the SRM which produce maximum of electromagnetic torque or minimum of torque ripple coefficient at the constant copper losses in [79]. A. Bentounsi has been presented a user-friendly numericalanalytical procedure by using Maxwell and Matlab software to design and optimize the geometrical parameters of a 6/4 SRM in2016. In [80] we have also examined the problem of choosing the conduction angles for accomplishing optimal control of SRG connected to a converter.

A.Fleury et. all. in 2012 has been presented an analysis about the mutual inductances of Switched Reluctance Generators. Mutual inductances profiles were presented pointing that they magnitude is greater than expected, contradicting previous related studies [81]. A convenient and nondestructive method for the measurement of Young's modulus of stacked lamination in electric motor stators is introduced by Zhangjun Tang et. all. In 2003. It shows the importance of Young's modulus in the calculation of stator resonant frequencies. The commonly used Young's modulus value is not appropriate for the calculation of resonant frequencies in the motor without a frame, however it produces lower errors for the motor with frame [82].

In [83] Senad Smaka in 2013 analyzes the effect of design parameters on the torque generation of the SRM 8/14. Design parameters were changed individually. To analyze the simultaneous effect of design parameters on the different characteristics of the machine, it is necessary to conduct the optimization. The method and results of design optimization of the SRM 8/14, which is currently performing, will be presented elsewhere. Balaji Mahadevan in 2015 has been investigated the influence of geometrical parameters that alter the pole face shape on the torque profile of SRM [84].

II. Different Torque Ripple Reduction Methods In Srm
2.1. Use of torque/rotor angular position/ current of SRM for its drive control

For determination of torque/current/angle characteristics of SRM under control a self-training technique has been used in [6]. This technique is suitable for very smooth operation over low speed. The self-training tests are performed before fixing the drive. Then an estimator software generates a table of phase current versus rotor angular position and torque by interpolation and inversion of the given test data. This data has been already stored in a memory and used on-line by the controller. This technique lasts a few minutes and computation and number of carried out tests are considerable. Some tests need sequence approximates or predictive techniques in order to generate precise result. To detect the rotor, position sensor is used.

In [7], test data is obtained by a modified linearize and decouple (LD) technique and stored in a EPROM memory as a table. A bi-cubic narrow band interpolation technique is used to model the data. By this method, peak and mean current are reduced. Meanwhile, the method causes the improved dynamic operation of inverter power switches. Also the speed ripple which in fact reflect the torque ripple are reduced. However, this method is applicable over low speeds. In addition to the memory, this technique needs EPLD and two D/A converters for control purpose.

In [8], a bi-cubic narrow band interpolation technique has been applied to estimate the torque from the flux-linkage/current/rotor angular position characteristics obtained by test. In this method, coefficients of the polynomial functions are calculated off-line by an interpolation (bi-cubic narrow band fitting algorithm) of the flux-linkage/current/rotor angular position characteristics and stored in a control processor memory. Internal voltage of SRM and measured current by current sensor are used to estimate the flux-linkage by integration. The third-order polynomial whose coefficients were already calculated, the rotor position is estimated using the obtained current and flux-linkage. The evaluated polynomial, flux, current and angular position are finally used to estimate the torque versus angular position. The estimated output torque is then compared with a reference and the result is fed to a current regulator in order to generate appropriate phase current of the motor. As a

result, the torque ripple will be lower using the suggested controller. The scheme of regulating and minimizing the torque has been shown in Fig. 1. This method has no advantage of overlapping the developed positive torques of two adjacent phases for minimization.
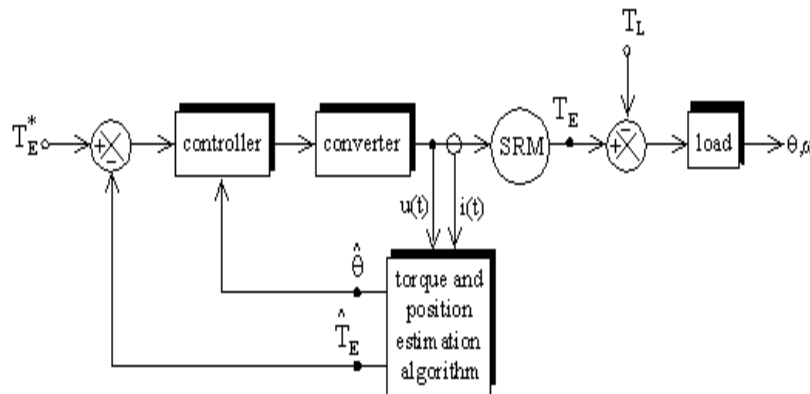

Fig. 1. Scheme of torque regulating and minimizing [8].

2.2. Optimizing and generating appropriate phase current for drive system

A method has been introduced in [9] based on the optimal curve of phase current in the conduction period of the extended overlapping of two phases in which instantaneous torque control is applied. The procedure is the torque control based on the tracking a counter for each phase of SRM as such that the summation of the developed torques by each phase is constant and equal to the desirable T_{ref} torque. A counter function $f_T(\theta)$ is defined as follows:

$$T_{total} = T_{ref} f_T(\theta) \qquad\qquad (1)$$

$$f_T(\theta) = \sum_{K=1}^{n} f_K(\theta) = 1,$$

where f_K is the counter function for *K*-th phase. The counter function for a phase is non-zero when the slope of inductance is positive. The effective factors in performing the suggested algorithm include torque/current/angular position characteristics, slope of the counter, and overlapping angle over simultaneous conduction of phase and current regulation algorithm. The algorithm is responsible up to the base speed and for performing controller the rotor position feedback from encoder is required. However, assumption of linear magnetization characteristic affects the performance of the method.

In [10], torque ripple have been minimized by generating current based on advanced control theory (fuzzy-logic). Due to the dependency of torque on the current (rotor position-dependent), current modulator based on the fuzzy-logic an integer term is added to the reference current. This modulator takes rotor position and torque error as inputs. Then the modified current passes other control blocks in order to regulate rise/drop of the current rate. The output of this block is the final modulated current which is sent to the stator winding. To perform the algorithm, the on-line measurement of the electromagnetic torque and rotor angular position are necessary. In this method, the reference current is optimized by FFT through forming optimization problem and solving it by Lagrange coefficients method.

On the other hand, modulator takes the position and normalized value of the torque (difference of the torque of motor and the desirable torque divided to the desirable torque) as input and the current correction term is given to the output. This value is multiplied by confidence factor (α) and the gain value and the result is added to the optimized reference current of SRM. In order to take into account the non-linear effects, the obtained value passes a clipper. Finally, this value is modified considering the increase or decrease rate of the current by fuzzy extraction mechanism and the final value is given to the motor winding. The obtained results show that the peak-to-peak of the torque ripple decreases from 40% to 15% and average torque error from 20% to 5%. The rotor angular position was obtained by encoder. Fig. 2 shows the current modulation based on fuzzy-logic.

In [11], the output signal of a neural-Fuzzy block of compensator as a function of position and load current is added to the output of a PI speed controller in order to reduce the oscillations and consequently the torque ripple through reshaping the phase current.
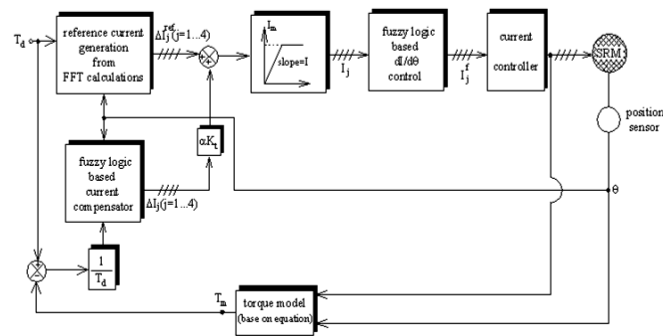
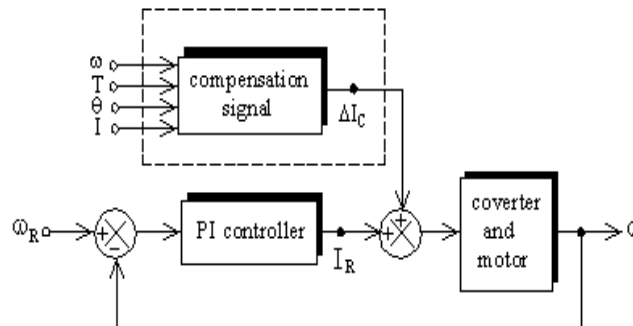**Fig. 2.** Current modulation based on fuzzy-logic [10].

Fig. 3. Diagram of proposed SRM torque ripple compensation scheme [11].

Speed or acceleration variable is preferred for Neural-Fuzzy on-line training because torque measurement is difficult. However, for off-line training it is appropriate to use torque error. The training trend consists of adjusting resultant rule by a combined training algorithm; it means back-warding and minimizing the least squares. The training data are obtained from steady-state simulation.

The dc component is deleted from the torque signal in every training iteration as such that only the ripple remain. Then, these torque ripple data are tabulated versus mean value of PI output reference current and rotor angular positions. This set of data passes the training algorithm, as such that the torque ripple are justified as information error for each pair of current-angle. The output of the neural-Fuzzy compensator is then adjusted to reduce the error and this process continues until the minimum of ripple places in the permissible ranges. Of course, it is noted that using membership bell shape functions leads to a better results compared to the triangular shape function in reducing the harmonic components.

In [12], a compensation mechanism as a closed-loop control is employed using a Fuzzy-logic controller and an adaptive neural-Fuzzy deduction (induction) system (ANFIS), in order to obtain optimal phase current waveform by compensating the phase current which finally reduces the torque ripple. The controller provides a smooth torque up to the base speed. Also, the controller is robust against the errors related to the position data from the sensor. Therefore, cheap position sensors are used. Fig. 4 shows the block-diagram of the SRM drive system with compensator of Fuzzy reference current and ANFIS. The important feature of Fuzzy-logic current compensator (FLCC) is that when there is a load or speed change, it is capable to adapt with this new operating point and searches for minimization of the required torque ripple.

Extension of simple and effective algorithms has been given in [13] in order to control the fixed torque of SRM. To do this, phase reference current waveforms for particular values of torque are determined and phase voltage curve is sequentially generated to effectively track these waveforms by the related stator winding. In two control design stages, iterative control training principles are used. Firstly, proper primary current waveform is generated as a primary waveform by iterated modifications with starting the iteration from traditional rectangular current profile. Secondly, the voltage profile affects stator phase voltages for tracking the desirable current waveforms trained iteratively. A bi-level controller has been used for torque control and it consists of (i) a forward-fed static compensator and (ii) a current controller. The compensator converts the desired numerical torque T_d into a desired current vector having for components I_j (j=1, 2, 3, 4). The current controller estimates proper phase voltages in order to affect the winding as such that the real current vector Im consisting of 4 current components I_j follows desired current vector I_d. Fig. 5 presents the schematic of this controller.

Meanwhile, compensator training process is carried out under motor static conditions while for current controller; controller operates under dynamic conditions in order to compensate the system delay. In [14], reforming the phase current method is used during the commutation period. The slope of the phase current over reference current switch-off period is controlled adaptively in closed-loop considering ripple information obtained from the speed signal. Fig. 6 shows the structure of the suggested controller.
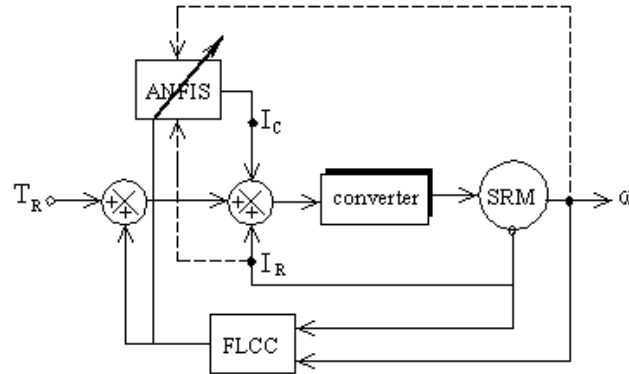
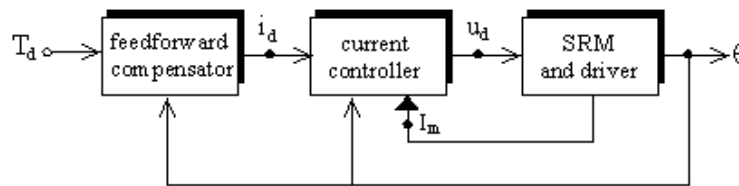**Fig. 4.** Block-diagram of SRM drive system with fuzzy reference current and ANFIS compensator [12].
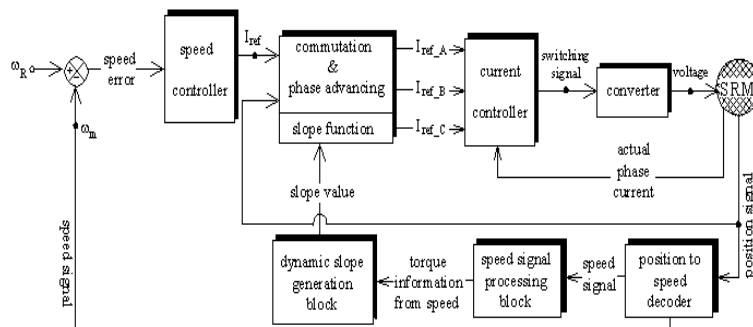

Fig. 5. Schematic of controller [13].

Fig. 6. Structure of the suggested controller [14].

The initial starting slope of the reference current is obtained using torque/current/rotor angular position characteristics by FEM. An algorithm for generating dynamic slope has been also presented. In fact, slope function operates as a compensator for external controller. The suggested controller is independent of the motor characteristic. Also, there is no a complicated algorithm for execution and consequently the computation time is short. In [15], a suggested algorithm has been used from a simplified model adaptively. Clearly, this consist of dynamic estimation of low harmonics combined by undefined load torque and ripple in the developed torque and adding proper terms to the current command to conceal these harmonics. The control structure consists of two stages: 1) given reference torque, which is converted to the excitation current and 2) closed-loop compensator, which supplied the reference torque. This algorithm diminishes the impacts of the modeling errors and considerably reduces the computations related to accurate but complicated use of torque/current waveforms. The controller also combines waveform simple parameters by dynamic estimation of low harmonic components from resultant torque error for torque ripple reduction. This needs encoder and DSP.

A method has been introduced for minimization of steady-state ripple at low speeds, which is efficient and inexpensive and does not require motor specifications [16]. However, it needs feedback of torque ripple

signal. The proposed trend permanently conceals torque harmonics by injecting following harmonic terms to the demand current signal:

$$I(\theta) = [\sum_{i=1}^{n} A_i \sin(K_i\theta + P_i)], \qquad (1)$$

which produces an additional torque equal with opposite sign of normal excitation case. Torque variance is used as the best method for determination of torque quantity.

In [17], the online simplex optimizing, which had been previously used to set the injected current harmonics to reduce torque ripple at low speed, has been explained and extended for higher speeds. The proposed method applies control of the switching angles. The method has been shown to be effective in reducing steady-state torque ripple and giving a suitable feedback signal to torque ripple, over the full speed range. The investigated method can also be used to minimize other undesired effects, such as acoustic noise.

In [18], a speed controller design has been presented for a SRM in order to achieve the minimum torque ripple and high control performance**.** In this method convertor is designed for soft chopping. In this method speed control loop of SRM drive includes a PID controller and a switching algorithm which determines turn-on and turn-off angles corresponding to each phase of motor. An optimization algorithm is defined and the corresponding parameters are optimized using a Genetic Algorithm (GA). This algorithm optimizes the turn-on and turn-off angles of each phase, the parameters of PID controller in transient state and parameters of PID controller in steady-state. The parameters of PID controller in steady-state are considered to reduce the torque ripple. Also, GA simultaneously obtains the optimum parameters of three nonlinear gains considered for fuzzy switching between the two PID controllers.

In [19], a new method minimizing torque ripple of an SRM is proposed which is based on the control of the sum of the square of the phase currents. The method makes use of only two current sensor and analog multipliers. In addition, the sliding mode control (SMC) technique has been applied to speed control loop that compensates the low frequency oscillations on the output torque. The motor is assumed to be working in the linear region and the mutual inductances are taken into account. The torque is proportional to the square of the current. So, in this method the sum of squares of phase currents is used instead of the sum of currents : $I_{ref}^2 = I_1^2 + I_2^2 + I_3^2 + I_4^2.$ **.** It is assumed that only two phases can conduct current simultaneously. Therefore, only two current sensors are available to control sum of the square of the current. So, $I_1I_3 = I_2I_4 = 0$ then $(I_1 + I_3)^2 = (I_2 + I_4)^2 = I_1^2 + I_2^2 + I_3^2 + I_4^2$ speed control block-diagram by SMC is shown in Fig. 7.
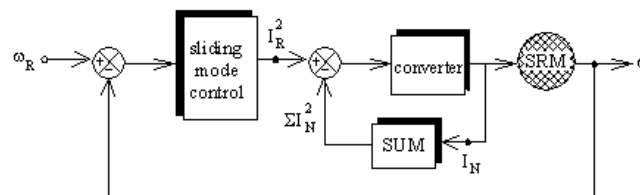

Fig. 7. Block-diagram for the speed control with SMC [19].

The sliding mode controller adjusts the value of the reference current to maintain the constant speed of motor. The algorithm is simple to implement and it does not need look-up table for saving motor characteristic or digital calculation. Also, the method reduces the ripple better than that of the PI controller and fuzzy controller. Moreover, this controller shows more robustness to external disturbances and it has better dynamic response. Another advantage is that it re-tunes itself when the command inputs are changed. In the investigated method a mechanical sensor for sensing the rotor position and a C-dump converter has been used.

Five new optimization procedures to minimize the torque ripple have been introduced in [20]. The main idea behind the new procedures is to optimize the phase current in the form of a positive "half-sine" waveform, which corresponds to the positive torque production of the motor, and to control this kind of waveform using a very small number of optimization variables (1-3 variables). Two optimization techniques, the simplex method and the GA, are adapted to these optimization procedures**.** It is noticed that the GA can better improved compared to the simplex method in which larger number of the optimization variables have been used. A comparison between the new procedures and the optimum harmonic current injection procedure using the same number of optimization variables shows a clear advantage of the new procedures from solution quality and calculation time. Also the new procedures use a cutting of the phase current. This helps preventing possible damages to the motor and also shorter computation time. Finally, due to this cutting stage, it is easier to produce the desired phase-current waveform.

New techniques which widely optimize the hysteresis current controller are studied in [21] and experimental results under closed-loop speed control with the modulated reference current data are presented. Three factors affect the performance of the hysteresis current controller in tracking the modulated reference current for zero torque ripple including the phase voltage, the step size and the hysteresis band. The phase voltage is reduced to minimize the rising rate of the phase current at the incoming reference current region. At the outgoing reference current region where the inductance is high, the current controller operates in the hard-chopping mode to force the current to decay fast. It has been found in this study that keeping the hysteresis band and step size in minimum value helps the current controller to track the reference current. The experimental results indicate that the torque ripple is reduced to the 5% of the desired steady-state torque. In this paper linear approximation of the inductance chart is used and also the flux and torque equations are assumed to be linear which affects the accuracy of the results obtained.

Based on the defining the commutation angle , at which two adjacent phases can produce the same torque for the same current, specific current references for commutation are proposed in [22]. The proposed method is theoretically able to eliminate the torque ripple due to the torque dip. In this method, the copper losses are reduced; however, the average torque is reduced as well.

2.3. Optimal turn-on and turn-off angles to control the drive system

Two controllers are proposed in [23] that determine the optimal turn-on and turn-off angles to improve motor efficiency and torque ripple. The suggested controllers are simple and do not affect the complexity of the drive. Since the knowledge of torque-angle-current characteristics or magnetization curves is not required they are easily implemented. If at θ_1(overlap starting point), the phase current reaches its reference value i_{ref} and θ_{o1} is angle of the magnetization area neglecting winding resistance and other fringing effect, the relationship between θ_1 , θ_{o1} and turn on angle is as follows:

$$\theta_{o1} = \theta_1 - \theta_{on} , \quad \theta_{o1} = \frac{L_u i_{ref} w_r}{V_{dc}} \qquad (2)$$

However, in order to get the optimum value, marginal effects and resistance should be taken into account. Therefore, (1) can be used as the initial value and optimum is obtained using flowchart of Fig. 8. After doing the calculations, turn off angle is equal to $\theta_c^{opt} = \theta_1 + (2\theta_{sk} - \theta_e)[1 - \frac{\theta_{o1}}{\theta_e}]$.

Block-diagram of turn-on and turn-off optimal controllers is shown in Fig. 9.
A method has been presented in [24] based on the optimal control of flux-linkage, through the firing angles, and according to demand load torque and rotor speed. A controller that determines the optimal turn- on and turn- off angles online is proposed. This controller does not affect the complexity of the drive and it is easily implemented, because the knowledge of magnetization curves is not required. Also in this method torque ripple reduced. Moreover, it provides smooth transition between the two modes of current control. The aims of 24] re obtaining the optimal firing angles in the single-pulsed
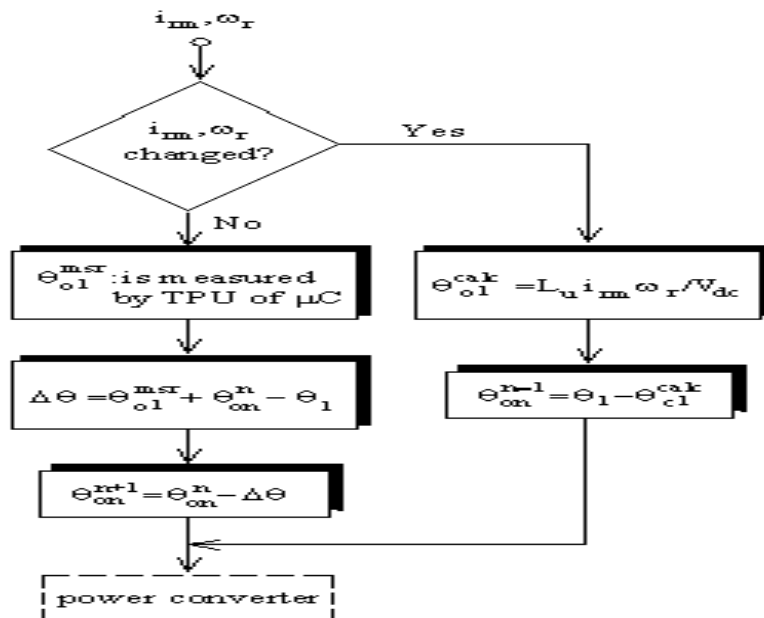

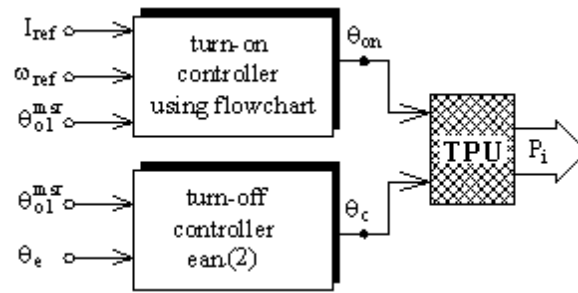**Fig. 8.** Control algorithm flowchart for turn-on angle fine-tuning [23].

Fig. 9. Block-diagram turn-on and turn-off optimal controllers.

Converter upper switches are controlled by a delta modulated current controller. To control converter lower switches, first produced optimal angles of the two controllers by means of microcontroller TPU are interpreted and then lower switches are controlled by signals P_j generated through TPU. This design is suitable for both low and high speed.

A method has been presented in [24] based on the optimal control of flux-linkage, through the firing angles, and according to demand load torque and rotor speed. A controller that determines the optimal turn- on and turn- off angles online is proposed. This controller does not affect the complexity of the drive and it is easily implemented, because the knowledge of magnetization curves is not required. Also in this method torque ripple are reduced. Moreover, it provides smooth transition between the two modes of current control. The aims of [24] are obtaining the optimal firing angles in the single-pulsed mode

mode. By defining $C_\lambda = {\theta_{o1}}/{\theta_{e1}}$ as a correction parameter, which is fixed and not under influence of saturation, it is used as a optimal condition to determine the firing angles and maximum efficiency in the single-pulsed mode. The following values are obtained:

$$\theta_{off}^{opt} = \theta_{1u} + (2\theta_{sk} - \theta_{e1})(1 - C_\lambda)$$

$$\theta_{on}^{opt} = \theta_{1u} - C_\lambda . \theta_{e1}$$

The optimal peak flux-linkage of single-pulsed operation is derived as follows:

$$\lambda_c^{opt} = \left(\theta_{iu} - \theta_{on}^{opt}\right)\frac{V_{dc}}{C_\lambda . \omega_r} \qquad (3)$$
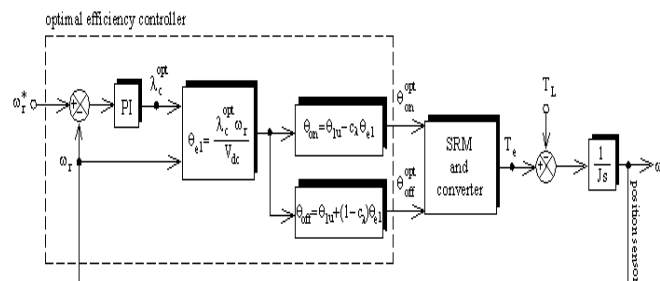

Fig. 10. Block-diagram of the optimal efficiency SRM control system in single-pulse mode [24].

The optimal current commutation control, which is based on optimal off-line selection of switching angles, has been presented in [36]. This control approach is performed with two different criteria: 1) the maximum electromagnetic torque and 2) the minimum electromagnetic torque ripple. The first criterion is adequate for high-speed process, while the second one is appropriate for lower speeds, where torque ripple can lead to undesirable speed ripple. To calculate the off-line optimum fire angles, just like real time implementation, a model based on the two following equations is used:

$$\Psi(\theta, i) = l_c . i + l_\theta(\theta).\text{sat}(i) \qquad (4)$$

$$T(\theta, i) = \frac{dL_\theta(\theta)}{d\theta} \int_0^t \text{sat}(i)\, dt \qquad\qquad (5)$$

Nonlinear functions $L_\theta(\theta)$, sat(i), as well as its derivatives and integrals are calculated from torque characteristics measured at standstill.

Optimum values of firing angles in a form of look-up table are stored in microcomputer memory. A sensor is used to obtain the position and the experiment is performed on a high-speed SRM. Applying position sensor for rotor position and DSP microprocessor control system equipped with FPGA module, increases the proposed scheme cost.

An optimization technique for commutation angles has been introduced in [26] which is based on FRM to maximize torque per current ratio. The proposed method is also adequate in improving the torque ripple. In the FRM method, flux density is divided into two normal and tangential components. Then, these two components, in points located in the middle of distance between the stator and rotor poles (contour), are calculated as follows:

$$B_{nk}(i, \theta_r) = i h_{nk}(i, \theta_r) \qquad\qquad (6)$$

$$B_{tk}(i, \theta_r) = i h_{tk}(i, \theta_r) \qquad\qquad (7)$$

In these equations, & are the normal and tangential basis functions which are calculated using truncated Fourier series expansion at each point on the contour. Having the flux-linkage density, torque and inductance can be calculated. According to the voltage equation used to model SRM, we have

$$V_j = R i_j + L_j(i, \theta) \frac{di_j}{d\theta} + \omega i_j \frac{dL_j(i, \theta)}{d\theta} \qquad\qquad (8)$$

For known position and current $L_j(i, \theta)$ and $dL_j(i, \theta)/d\theta$ can be quickly and precisely updated in voltage equation. Solving the differential equation by software, the optimum current is achieved and the value of torque is then calculated. Due to difficulty of torque control at high speeds, an iterative optimization process is carried out. The optimization constraints need to be properly defined searching for the optimal commutation angles in maximum torque per amp at various speeds. Also, commutation angles should be iteratively calculated to search for the minimum of excitation current required for each specific operation point (torque and speed). Before applying the optimization constraints, commutation angles need to be defined as optimization variables. Having two optimization variables, conduction angle (15 degrees) and turn-on angle, calculated repetitively to search for the minimum of excitation current, turn-off angle is also determined. At higher speeds, the overlap angle is also considered to calculate the turn-off angle, thus

$$\theta_{off} = \theta_{on} + \theta_{dwell} + \theta_{overlap} \qquad\qquad (9)$$

Using this approach, the excitation current amplitude decreases and the torque ripple are reduced. Moreover, iterative optimization implementation by FRM requires shorter computation time compared to FAM, which is considered an advantage. A neural network based controller is used in [27] to obtain the optimum turn-on and turn-off angles to minimize the torque ripple and speed ripple. Block-diagram of the proposed controller has been shown in Fig. 11. This method simplifies the control of SRM and reduces the complexity and cost of the drive.

2.4. Torque-sharing function technique

A novel and simple nonlinear logical torque-sharing function (TSF) for a SRM drive is proposed in [28] that use nonlinear TSF to change currents in two adjacent phases during commutation, so that efficiency and torque ripple in an SRM drive can be considerably improved.

The incoming phase produces the majority of torque and the current of outgoing phase is decreasingly controlled by the logical condition.
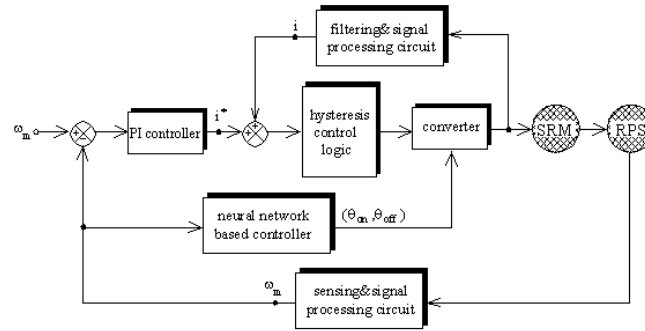
Fig. 11. Block-diagram of neural network-based controlled SRM [27].

Due to the same switching condition in an unregulated phase and the reduction of commutation period in the proposed control method, the number of switching can be significantly reduced, and hence, the switching loss can be reduced. A two-phase regulation mode is employed in the novel nonlinear TSF. In order to include nonlinearity in torque control and decrease the tail current at the end of commutation, the current of the incoming phase needs to be controlled in an increasing manner, and at the same time, the outgoing phase current should be tracked on an opposite direction; so that torque sharing between two phases is smoothly achieved with a minimum current crossover. Comparison between the total torque chart of the proposed TFS method with the two conventional methods clearly shows superiority of the proposed method in reducing torque ripple. At low speeds the efficiency of the proposed method is better than other traditional methods (linear TSF and sinusoidal TFS). At high speeds, efficiency of the three methods is similar. For practical implementation of DSP, analog to digital converter and encoder for positioning are required. In addition, this method needs the characteristics of torque-angle- current of the motor.

Two improved torque-sharing functions to implement torque ripple minimization (TRM) control have been presented in [29]. These functions depend on the turn-on angle, overlap angle, and the expected torque. This study shows that for a given torque, the turn-on angle and the overlap angle have significant impacts on the speed range, maximum speed, copper loss, and efficiency. Here, GA has been used to optimize the turn-on angle and the overlap angle at various torques operating under the proposed TRM control in order to maximize the speed range while minimize the copper losses. The fitness function is expressed by two optimization objectives with a weight factor to maximize the speed range and minimize the copper losses. Four torque-sharing functions namely linear, cubic, sinusoidal and exponential are studied. If providing maximum speed range is the only evaluating target, exponential TSF is the best selection. However, if the minimum copper loss is the optimization target, any of the four TSFs is a reasonable selection. When the weight factor is equal to 0.5, the cubic or sinusoidal TSF is the best choice. A fast and accurate method (least-square polynomials) is proposed to compute the optimal turn-on and overlap angles. Fig. 10 depicts torque ripple control scheme using TSF model.

A torque control scheme using modified TSF for high speeds has been presented in [30]. Because of a short commutating duration in the high speed region, the negative torque caused by the tail current leads to high torque ripple. In order to reduce the torque ripple, the proposed modified TSF compensates the negative torque of the tail current in the active phase winding. The torque references corresponding to each phase have additional compensating term to reduce the torque ripple, and the compensating value depends on the tail current of the inactive phase winding. Torque sharing in the overlap region is done considering two different modes.
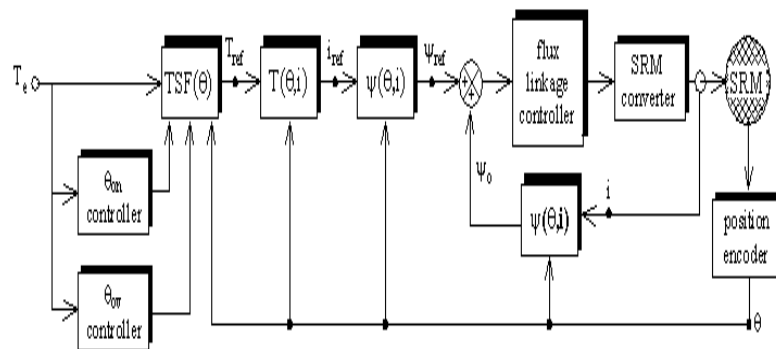

Fig. 12. Scheme of TRM control using TSFs [29].

In the general speed region, switching of the two phases is controlled by the torque error, but the outgoing phase switching is limited in the high speed region. In order to reduce the tail current in the high speed region, the outgoing phase is fully turned off, and the torque error of the outgoing phase is compensated by the incoming phase during overlap region. In this method, rotor position is determined using a non-contactable magnetic sensor. To reduce the ripple, an SRM with continuous non-uniform air gap has been used. Experimental and simulation results show that applying the proposed method, torque ripple can be controlled well.

The optimization criterion of TSF for torque-ripple reduction in SRM, providing low copper losses with acceptable drive performance, has been discussed in [31]. In proposed method, the reference current waveforms are directly derived from the reference torque using a reliable analytical expression. In this study two types of the proposed TFSs (defining new equations) and two conventional (sinusoidal and linear) TSFs are optimized for the SRM drive, and their control performances are then compared through the torque-ripple control applications. The two proposed TFSs can improve the drive efficiency, development of the possible torque-ripple-free speed range and reduction of the peak current requirement compared to the two conventional types. Note that the copper losses in an SRM drive depends on TSF type and TSF parameters such as turn-on, turn-off and overlap angles.

2.5. Modern method of neural network

An SRM torque ripple reduction scheme using a two-dimensional (2D) B-spline neural network (BSNN) has been proposed in [34]. BSNN is a kind of associative memory neural network which is suitable for online nonlinear adaptive modeling. Closed-loop control can be implemented by using on-line torque estimator. Due to the local weight updating algorithm used for BSNN, an appropriate phase current profile for torque ripple reduction can be obtained on-line in real time. It has good dynamic performance with respect to the changes in the demand torque .This scheme does not require high-bandwidth current controllers.
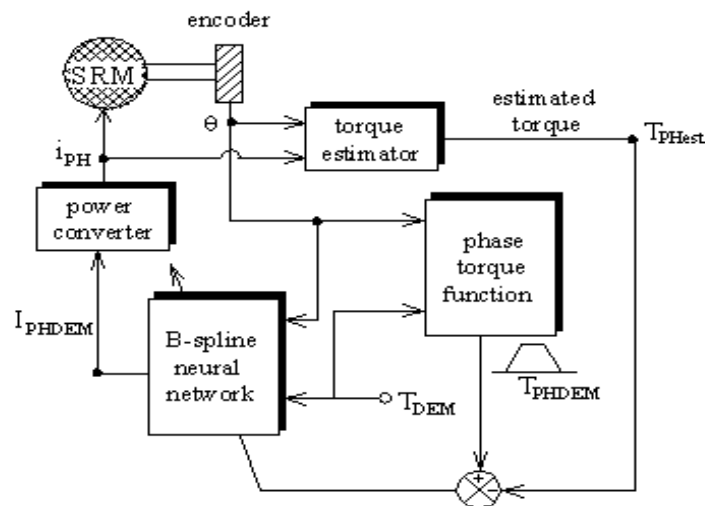

Fig. 13. Torque ripple reduction diagram [34].

Block-diagram of the proposed scheme is shown in Fig. 11. To practically implement this scheme, a digital signal processor for on-line estimation of the torque and ripple reduction, evaluation module to implement the current controller and an encoder to get the position are required.

Torque model and the inverse torque model have been developed in [35] based on BP neural network model of Levenberg-Marquardt algorithm using the measured static torque characteristic. Then torque ripple have been minimized by optimum profiling of the phase current based on instantaneous torque control. Also an efficient commutation strategy for minimizing torque ripple while avoiding power converter voltage saturation over a wide speed range of operation has been proposed. The phase used to produce the desired torque is controlled by the hysteresis current controller.

The desired phase torque in this interval is obtained subtracting the sum of the other phases torque from the total torque command. Here, the generated torque by the other phases is estimated using BPNN model of SRM torque. Then, the SRM inverse torque model built by BP neural network is used to generate a phase current command. The torque ripple minimization can be achieved by optimum phase current profiling.

2.6. Modern method of fuzzy-logic

A fuzzy-logic-based turn-off angle compensator has been proposed in [36] to reduce the torque ripple in SRM. The turn-off angle is automatically changed for a wide range of motor speed to reduce torque ripple. Block-diagram of the proposed compensator is shown in Fig. 14.
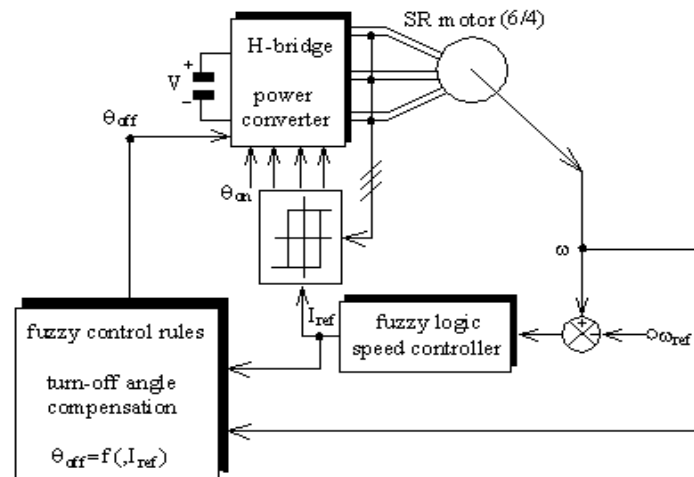

Fig. 14. Block-diagram of the proposed compensator [36].

Two procedures are used to measure the torque smoothness: 1) The variance value of speed error variation and 2) Its frequency spectrum. Analyzing power frequency spectrum diagrams and also table of variance values before and after compensation, improvement in the performance of the drive system is clear in reducing speed and torque ripple. The proposed compensator also has the ability to reduce the noise and machine vibration. In addition, no torque signal has been used in this scheme that increases the simplicity and reliability of the compensator.

A high performance drive based on high speed and low speed dynamic observer (HSO and LSO) has been introduced in [37]. The dynamic observer estimates the rotor position and speed over wide speed range using currents and phase voltages. In this approach, observer gains are corrected on-line using fuzzy-logic hybrid algorithm (FLHA) regarding estimation errors. In addition, a fuzzy-logic current compensator (FLCC) has been presented to reduce torque ripple. In the torque reducing regions, the FLCC injects additional current into each phase. Simulation results show that the proposed scheme estimates the rotor position and speed with high precision for all speeds (near zero up to the rated speed). Also, FLCC minimizes the torque ripple and reduces the speed estimation error. Some advantages of this drive are robustness, high reliability and very good performance in the steady-state.

A novel adaptive TSK-fuzzy controller (ATSKFC) has been presented in [38] to regulate the speed of an SRM. The proposed controller comprises two parts: 1) a TSK-fuzzy controller and 2) a compensated controller. In this paper, the TSK-fuzzy controller is the main controller, which is used to approximate an ideal control law. The compensated controller is designed to compensate the approximation error between the TSK-fuzzy controller and the ideal control law. The parameter variations and the external load of the SRM drive are taken into account to ensure the robustness of the proposed scheme.

An on-line tuning methodology based on Lyapunov is utilized to adjust the parameters of the ATSKFC, so that the stability of the control system can be guaranteed. Also, three control schemes namely ATSKFC, fuzzy control and PI speed control are experimentally investigated and their results are compared with each other. Configuration of the proposed scheme is presented in Fig. 15.

Here, input variables of TSKFC are the speed error and the speed error variation and its output is designed to obtain U_{TSKFC} control law. Three experiments are presented in this paper. Analyzing the experimental results of different controllers in experiment 1 with three different reference speeds, the proposed scheme clearly has a lower speed error. It is clear in experiment 1 that fuzzy controller performs well in the steady-state but shows larger speed error in the transient mode. The PI speed controller also works well, when it is well tuned; however, the PI speed control does not perform satisfactorily over a wide range of speed. Unlike the PI speed controller, the proposed ATSKFC can handle a wide range of speeds because its control strategy is self-tunable.
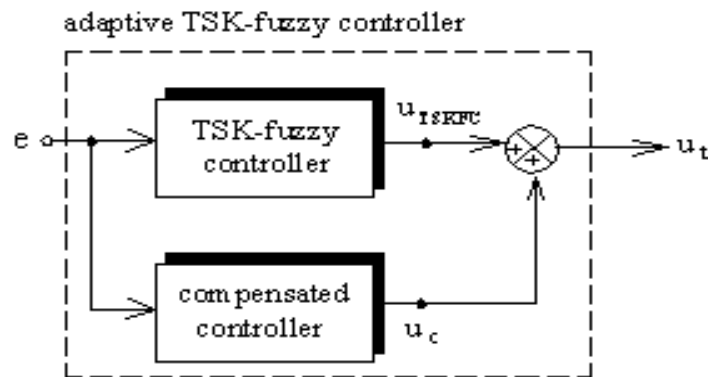
Fig. 15. Configuration of the proposed ATSKFC [38].

In experiment 2, when SRM handle the external load torque disturbance in the steady-state, the proposed method can react against disturbance injection much more effectively and quickly.

Finally, in experiment 3 under full-load condition, the proposed method offers (in the minimum error speed and torque ripple) a more outstanding performance. Totally, the ability to adjust the speed over a wide range, ability of dynamic tracking and robustness of the proposed method are better than that of the two other methods. Moreover, the torque ripple of the scheme are acceptable and limited.

A tuned fuzzy-logic speed controller (TFC), with output tuning factor based on fuzzy-logic reasoning has been designed and simulated for SRM drive [39]. The TFC uses the speed error and change in speed error as inputs and generates an equivalent control term (reference current), which improves system performance in steady-state. In this method, SRM non-linear modeling is based on the look-up tables that are obtained from FAM. The TSF performance has been compared with other control methods such as PI and FLC. It is proved that this method is superior to conventional approaches in several aspects including the reduction of ripple. In this approach, a sensor is used to measure position.

A new control scheme has been proposed in [40] that aims at minimizing periodic speed ripple originated by torque pulsations, so that the steady-state speed response of the drive system is improved. The outer loop speed control is performed by a PI controller in conjunction with a fuzzy controller. The PI speed controller provides the main reference current. In steady-state, the error signal between the reference speed and actual motor speed is fed to the FC, so that it generates the compensation term that is added to the main reference current and minimizes the speed ripple. PI current controller is used in the inner control loop to generate the control voltages.

Torque characteristics and flux-linkage are obtained from FAM and stored as a look-up table. In SRM dynamic model, look-up tables are used to estimate the current and torque, when the input voltage and rotor position are available.

2.7. Torque control
2.7.1. Torque controller design

A controller for an SRM has been developed to minimize torque ripple [42, 43]. This controller is robust, and can be easily implemented in standard digital hardware (DSP). Also, a new, simple and efficient commutation strategy is proposed. The objective is to design a cost effective controller to minimize torque ripple which can be adaptively updated in real time. The algorithm is suitable for both low and high speeds and does not require pre-calculated flux or current profiles. However, the computation time of the control cycle increases. Block-diagram of the controller has been presented in Fig. 16.

The function of the electronic commutator is to designate the appropriate phases for torque development and commutation. The algorithm used by the electronic commutator maximizes the overlapping conduction region in which more than one phase can be used for positive torque generation. The torque controller uses measured phase currents to estimate the torque produced by each phase, except the one designated by the electronic commutator. The suitable phase torque is obtained extracting the total reference torque. The command torque is then transformed to current commands and is fed to an external hysteresis controller that drives the power converter. The proposed approach, together with a new commutation scheme compensates the non-ideal operation of the remaining phases. A DSP is required to implement controller and also an encoder to obtain the rotor position.
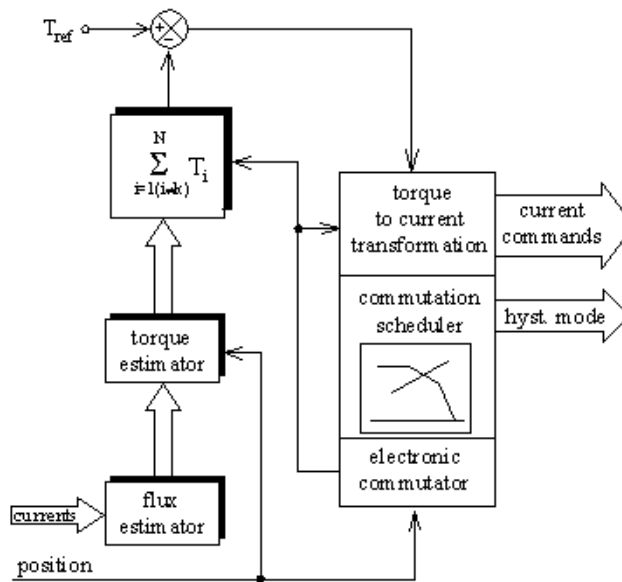
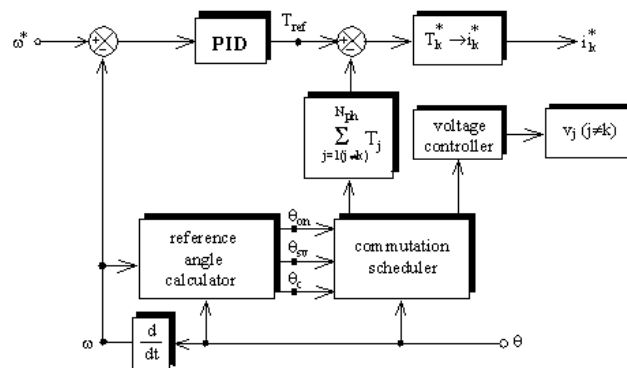**Fig. 16.** Block-diagram of torque controller [42, 43].

Fig. 17. Block-diagram of hybrid controller [44].

In addition to a review of the previous approaches adopted to minimize torque ripple, [44] has presented a hybrid controller to minimize the torque ripple. The proposed method is based on merging the past developed techniques.

The concept of torque sharing over an extended region is merged with the balanced commutator approach to minimize torque ripple. The ripple minimization over a wide range of speed is achieved varying the central commutation angle θ_C between θ_C^i and θ_C^λ as a function of speed. The controller structure is shown in Fig. 17.

2.7.2. Instantaneous torque control

An on-line instantaneous torque control technique for an SRM operating in the saturation region has been presented in [45]. The proposed methodology realizes the instantaneous output torque controlling for each excited phase by regulating its associated co-energy in order to follow the co-energy profile. The design of the proposed controller is simple when compared to that of traditional current controllers. The reason is that in the proposed methodology, the parameters of the feedback controller are independent of the motor parameters in the analysis of the co-energy control system. Smooth shaft torque is obtained by torque sharing among the active phases during commutation. The proposed controller structure is presented in Fig. 18.
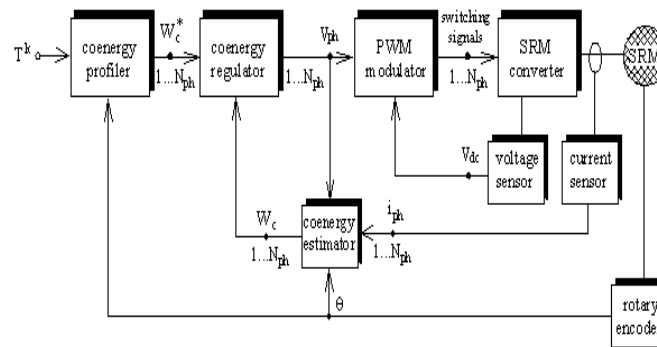
Fig. 18. Structure of instantaneous torque controller for SRM [45].

In this structure, the reference torque and rotor position are used to obtain the co-energy references W_C^*. Also, phase current signals, terminal voltage and rotor position are used to estimate co-energy to control it.
The co-energy can be estimated on-line without extensive knowledge of the motor magnetic characteristics. Simulation and experimental results shows that the proposed algorithm yields smooth output torque algorithm that follows the torque command well. In addition, it is obvious from the presented results that high-frequency torque ripple is reduced.

2.7.3. Direct torque controller
A novel Lyapunov function-based direct torque controller (DTC) to minimize of the torque ripple in an SRM drive system is reported in [46].
The DTC scheme avoids the complex process of torque-to-current conversion which is common in indirect torque control scheme. The traditional DTC scheme uses a hysteresis-type torque controller leading to a large amount of torque ripple when implemented digitally. The proposed controller is intended to take care of the nonlinear system dynamics of magnetic characteristics associated with accurate torque control using DTC scheme for an SRM drive system.
In the proposed Lyapunov function-based controller, the variable feedback gain is adopted using a heuristic technique. The stability of the proposed controller is ensured using the direct method of Lyapunov.
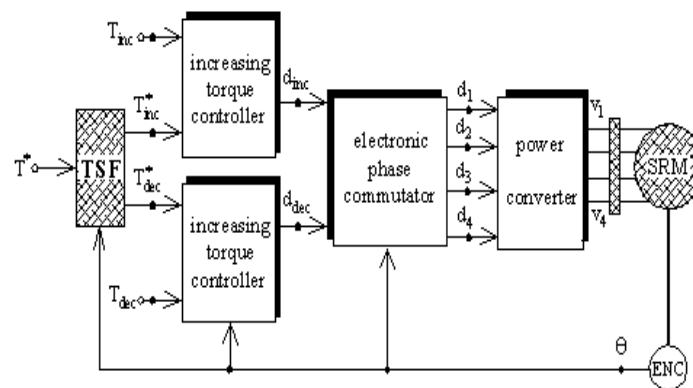The proposed control scheme is presented in Fig. 19.

Fig. 19. Schematic of proposed DTC scheme [46].

Comparing hysteresis torque controller and the Lyapunov function torque controller indicates that using Lyapunov function controller demand torque follows the reference torque more accurately. Ripple related to average torque is within the acceptable range and it is less than that of hysteresis controller.
A comparative study of DTC method with direct instantaneous torque control methods (DITC) and current profiling technique, for 3-phase SRM has been performed [47] shows that DTIC does require rotor position information or encoder. However, using DTC, higher phase SRM current is necessary to maintain constant flux-linkage in all situations of the rotor. This reduces the ratio of torque to current and diminishes efficiency as a result. Furthermore, using DTC approach, different flux-linkage references are required to produce the same torque at different speeds for optimum torque/ampere. Then a new DTC scheme has been proposed in which the voltage vectors are chosen, so that the current of the active phase is controlled to produce the desired torque and the current of outgoing phase is made to decay quickly. Thus, the torque/ampere is

improved reducing the conduction time of each phase. Also flux-linkage is maintained constantly only during phase current commutation to eliminate the need for rotor position information; thus the performance of this scheme is not very sensitive to the flux-linkage reference. Result shows that unlike previous DTC scheme, one reference flux-linkage can be used to produce the same torque at different speeds in this proposed DTC scheme. Comparing the resulted waveforms deduces that using proposed DTC method, phases conduct to a shorter period and less negative torque is produced compared to DTC method. As a result, ripple torque is also improved. Comparing the table of obtained results it is realized that:

1) Considering the minimum effective current, minimum phase current peak and maximum torque/ampere, the current profiling technique and then the proposed DTC scheme takes place,
2) DITC and the proposed DTC scheme have the minimum amount of switching transitions.
3) The torque/ampere is more sensitive to variation of reference flux-linkage in DTC scheme compared to the proposed DTC scheme.

2.8. Performance poly-phase

A bipolar excitation scheme for a mutually coupled SRM (MCSRM) has been proposed in [9] to reduce torque ripple that includes two excitation modes. A shift angle between co-energy profiles of the MCSRM under two excitation modes is studied based on finite element analysis (FEA). The bipolar excitation scheme reduces the torque ripple considering the shift angle. A comparison between the torques produced by the MCSRM under traditional single-phase unipolar excitation scheme, two-phase bipolar excitation scheme, and the proposed bipolar excitation scheme has been provided. A 6-phase MCSRM has been presented to develop the excitation scheme that makes it possible to excite the windings on opposite poles separately. If two adjacent phases are positively excited, the currents of the two phase windings in the same slot will have the same direction. The proposed scheme has two modes: In mode 1, only one pair of opposite phases is stimulated while in mode 2, two pairs of opposite phases are stimulated. Comparison of torque and torque ripple for the three types of stimulation has been presented in Figs. 20 and 21. As it can be seen, the proposed scheme has the highest average torque with the lowest torque ripple, with higher current; this plan shows the lower torque ripple in comparison with the two other schemes. The proposed scheme has a better performance at low speeds. Results show that iron losses in the proposed scheme are higher than that of the two other types (due to higher switching frequency). The copper loss is between the copper losses of the two other types and generally shows more losses than the two other types.
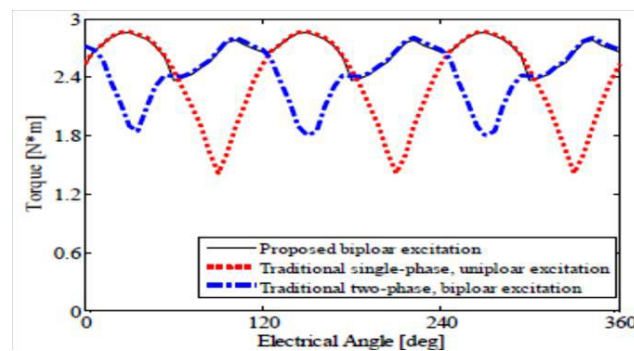

Fig. 20. Comparison of instantaneous torque waveforms under different excitation (I=10A) [48].
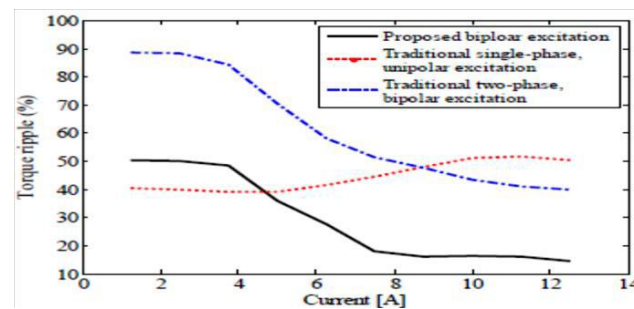

Fig. 21. Torque ripple of a 6/8 SRM under different excitation schemes with different current magnitude [48].

As it can be seen, the proposed scheme has the highest average torque with the lowest torque ripple, with higher current; this plan shows the lower torque ripple in comparison with the two other schemes. The proposed scheme has a better performance at low speeds. Results show that iron losses in the proposed scheme

are higher than that of the two other types (due to higher switching frequency). The copper loss is between the copper losses of the two other types and generally shows more losses than the two other types.

2.9. Changing geometry and structure of the motor

A proposal for a new stator pole face has been described in [49] which have a non-uniform air-gap and a pole shoe attached to the lateral face of the rotor pole in order to reduce the ripple. The effects of each design parameter are investigated using a time-stepping FEM. The parameters are optimized utilizing response surface method (RSM) combined with (1+1) evolution strategy. By optimizing the air-gap profile and pole shoe, the torque ripple is reduced to 23% of its value before optimization.

A two-phase 4/2 pole SRM used in a high-speed air blower is investigated in [50] and its pole shape is optimized to reduce the torque ripple. In order to produce a continuous output torque, the positive torque region is extended with an asymmetric inductance characteristic. The rotor shape is optimized with a reiterative optimization algorithm using FEA. The torque ripple is reduced (below 2%) developing positive torque area and non-uniform air-gap.

2.10. New converter design

Since the excitation time is very short compared to the general speed range of a high speed drive, the excitation current cannot be built-up sufficiently. Also, the demagnetization current can be easily extended to the negative torque region.

A novel four-level converter has been proposed in [51] to obtain a fast build-up current and a suitable demagnetization current. The proposed converter has an additional capacitor and an active power switch compared to a conventional asymmetric converter. The high voltage of the additional capacitor is applied to the phase winding in the fast excitation mode and the phase current decreases rapidly during recharging of the capacitor in demagnetization mode. In addition, an instantaneous switching angle detector separated by main digital controller is designed for precise switching angle control.

During high speed operation, rotor position error increases due to the constant sampling period of digital controller.

The proposed detector operates with optical encoder pulse and pre-set switching position regardless of sampling time. So, it determines precise switching pattern without any time delay. This converter has been shown in Fig. 22 for a three-phase motor.

In comparison with the asymmetric converter, using proposed converter, current in the excitation mode can be constructed faster and is reduced faster in the demagnetization mode.
Response time of the proposed converter is shorter, current peak, speed ripple and therefore, its torque ripple is lower. In addition the proposed converter drive efficiency is higher and its stable performance period is longer compared to the asymmetric converter.
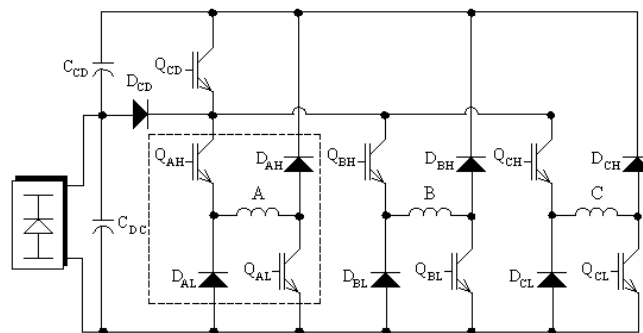

Fig. 22. Proposed three-phase four-level converter for high speed drive [51].

A new converter for SRM drive has been suggested in [52] which use one switch in each phase. The proposed drive reduces cost and increases motor efficiency. The negative torque and also torque ripple are largely removed in the proposed scheme. The topology of this converter has been show in Fig. 23. This converter operates only with one switch per phase and through the mechanism of coupling between the two windings, returns stored energy to the source. This converter has the ability to control phase currents separately.
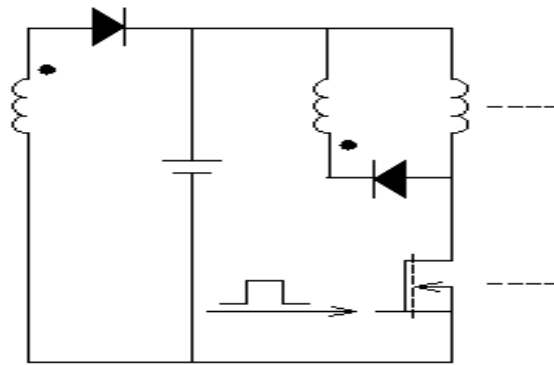
Fig. 23. Proposed SRM per phase converter [52].

2.11. New models and advanced algorithms

A modern control system for SRM drive has been presented on [53]. This control system operates based on computational model of mammalian limbic system and emotional processes (BELBIC) which decrease torque ripple as a drive speed controller. A novel and simple model of SRM drive control plant is achieved using the intelligent control system, which controls motor speed accurately and directly. There is no need to use any conventional controllers. Also, the proposed method is quite independent of the motor parameters. The proposed method is compared with a conventional PI controller and sliding mode controller as a nonlinear approach. A previously developed network model has been adopted as a computational model which mimics parts of the brain responsible for processing emotions. Two input signals exist in BELBIC, sensory input and emotional cues (reward signal) which are modeled as follows:

$$S = k_1 e + k_2 \frac{d}{dt} e + k_2 \int e \, dt \qquad\qquad (9)$$

$$R = k_1 \left| e \right| + k_2 \left| \int e \, dt \right| + k_2 \left| E \right| \qquad\qquad (10)$$

where e and E are the system error and controller output respectively. Gains $k1$-$k3$ and $K1$-$K3$ must be tuned in order to design a satisfactory controller. The purpose of BELBIC is reduction of the sensory input (1) regarding the reward signal. The reward signal specifies quality and satisfying level of the control process. The block-diagram of the new control system incorporating the emotional controller (BELBIC) has been shown in Fig. 24. The input of the emotional controller is the speed error and its output is the reference current. The reference current is compared to the actual stator current, and then generated current error is entered to the PWM inverter to generate gate pulses which fire the switches. Switches of each stator phase only are fired in the interval between on and off angles recognized by an angel definer. Rotor position is produced by an encoder.

A comparison between three types of control methods has been presented in Fig. 25 which corresponds to a step change in speed. They represent the faster dynamic response and lower torque ripple of the proposed method compared to SMC and PI methods.

Optimization process of SRM design has been carried out using a combination of Seeker Optimization Algorithm (SOA) and FEM in [54]. SOA is based on the simulating the act of human searching process and regards optimization process as a search of optimal solution by a seeker population.

The proposed algorithm has been also compared with GA. The results show that the optimized motor using SOA has a higher torque and efficiency with lower mass and torque ripple. The objective function satisfying both conditions of maximum torque and minimum mass, is a weighted sum of both objective
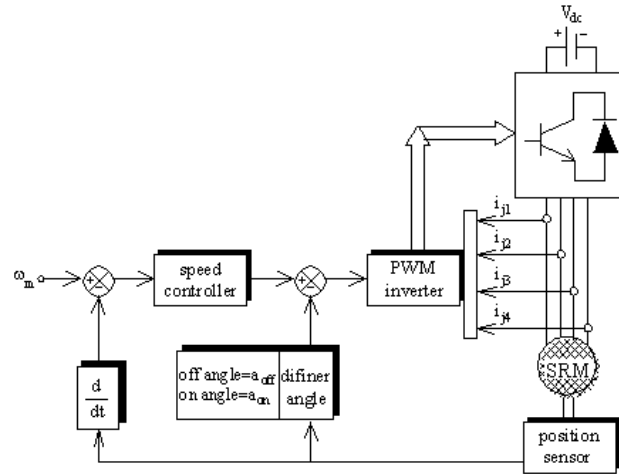
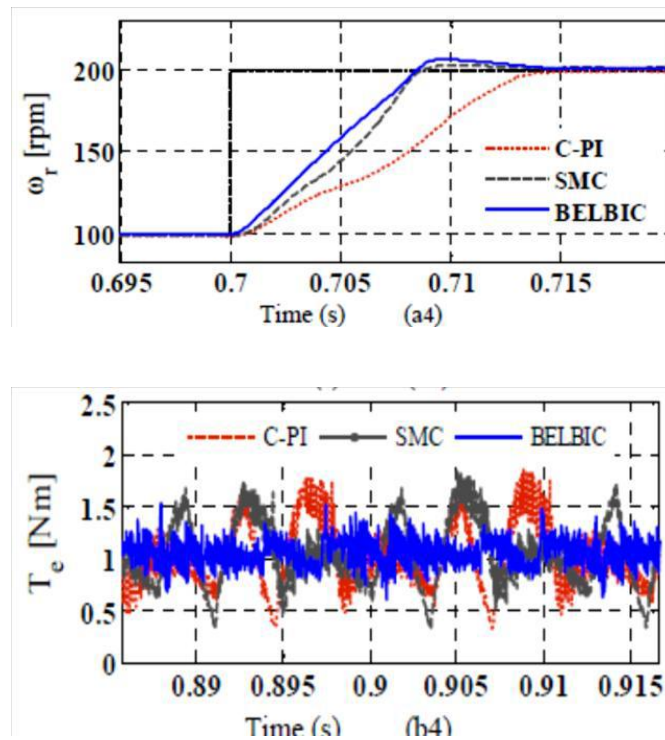**Fig. 24.** Control system structure of SRM drive [52].

Fig. 25. Simulation results, SRM speed control using BELBIC, C-PI & SMC; a) rotor speed; b) electromagnetic torque [53].

functions, *f(x)*, defined as

$$f(x)=P.\frac{T_{avgo}}{T_{avg}}+\frac{M}{M_0} \tag{11}$$

The purpose of the optimization is therefore to find the set of parameters **x** for which the value of the objective function is minimum. These parameters are the stator pole width, the stator yoke, the rotor pole width and the rotor inner radius. The investigated methods of the optimization include GA and SOA; however, the paper has focused on SOA. The results obtained from experiments and simulations show higher torque, lower mass and torque ripple of the SOA method in comparison with GA method. A comparison between torque curves of the two methods after optimizing the torque and mass has been shown in Fig. 26 which clearly shows higher torque in method SOA.

A control scheme for speed control of SRM has been presented in [55], which reduce the torque ripple using non-dominated sorting AG (NSGA-II). NSGA 2 algorithm is in fact modified version of the NSGA which relieves three problems associated with version 1.The control scheme includes PI speed controller in the outer loop and PI current controller in the inner loop along with control of turn-on and turn-off angles for the 3-phase SRM. The problem of obtaining the optimum values of proportional and integral gains for both speed and current controller along with the turn-on and turn-off angles are considered as a multi-objective optimization problem.

The objective is defined as minimizing the integral squared error (ISE) of speed and torque ripple. The results obtained by NSGA-II are compared and validated with real coded GA (RGA) with simulated binary crossover (SBX).
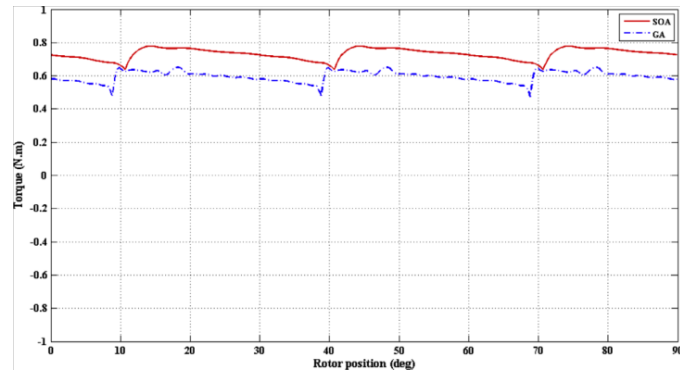

Fig. 26. Torque profile after 'torque and mass SOA optimization' compared with GA [54].

Assumptions are as follows:
1) Neglecting mutual inductances
2) Operation of the motor in the linear region of the magnetic characteristics

The block-diagram of SRM and NSGA-II along with controllers has been shown in Fig. 25. ISE corresponding to speed and current controllers are obtained as follows:

$$\text{ISE-Speed} = \int (w_{ref} - w)^2 . dt \qquad (12)$$

$$\text{ISE-Speed} = \int (I_{ref} - I_{pha})^2 . dt \qquad (13)$$

In this work, minimization of speed ISE and torque ripple can be considered as objectives and current ISE in the inner loop is considered as a constraint. The results reveal that NSGA-II based controllers give better performance in terms of smaller torque ripple and quick settling time compared with the controller based on RGA-SBX.

In [56], smart bacterial foraging algorithm (SBFA) is used to tune the coefficients of a PI speed controller for SRM drives considering torque ripple reduction. This method mimics the chemotactic behavior of the E. coli bacteria for optimization. The proposed algorithm is applied to a multi-objective function including both speed error and torque ripple. Results confirm the improved performance of the adjusted PI controller using SBFA in comparison with adjusted PI controller using standard BFA. The objective function can be written as follows:

$$J = \int_{t_{1=0}}^{t_2} k. \left| E \right| . dt + \int_{t-t'}^{t_2} \left| T_{ef} - T_e \right| . dt \qquad (14)$$
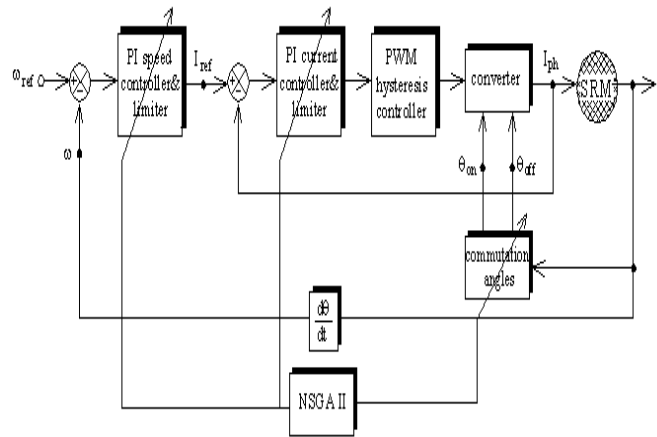
Fig. 27. Block-diagram of SRM with NSGA-II-based controllers [55].

where *K* and *E* are the constant value and the speed error, respectively, and T_{ef} is the filtered electromagnetic toque. The electromagnetic torque is calculated using a look-up table. As seen SBFA based PI controller reduces torque ripple, current ripple, their harmonics and the control effort. Furthermore, the proposed algorithm is based on a smart prediction method, unlike conventional methods which are random based (such as GA, PSO and AI) techniques.

Clearly the speed and torque ripple are lower using the SBFA method compared to BFA method.

III. Conclusion

This paper is a comprehensive overview of already proposed methods to reduce the torque ripple and acoustic noise of SRM. Among the discussed various current optimization processes, sliding mode control method (SMCM) and fuzzy intelligent technique (FIT) have provided better results. To store the characteristics of SRM and digital computation, the SMCM does not require a look–up table. Also, it has better performance than that of fuzzy and PI controllers in reducing the ripple; it has better dynamic response and more robust against external fluctuations. Online control method shows better results among the optimal fire angle control methods. Knowledge of the characteristics of torque-angle-current or magnetization characteristics is not required in this method. Moreover, it can be used at both high and low speeds. Results of the torque sharing function method, which is one of the most popular methods, is very good and satisfying. Paper [51] has the advantage that it does not require the characteristic of the torque-angle–current. In addition, two types of TSFs have been proposed which improves drive efficiency, develop the range of speed with free torque ripple and reduce the peak current requirement in comparison with the two conventional types.

Intelligence techniques such as fuzzy-logic, neural network, or a combination of these methods, have the advantage of using SRM non-linear models. Thus, more accurate results are obtained. Using fuzzy-logic as speed controller or controller which can work along PI speed controller has better and more accurate results than a single PI controller.

Another method is the use of neural networks which despite its complex nature shows better results than fuzzy-logic. To optimize and obtain the appropriate values of speed or current controller gains or both, methods and smart algorithms have been used recently. Apart from the method presented in [65], the results of the rest of methods are very good, satisfactory and have minimum torque ripple.

References
[1].   Lawrenson P J, J. M. Stephenson, P. T. Blenkinsop, J. Corda and N. N. Fulton,"Variable-speed switched reluctance motors", IEE Proc., Vol. 127, Pt. B, No. 4, July1980, pp 253-265.
[2].   Bryne J. V, O'Dwyer J. B. and McMullin M.F., "A high performance variable-reluctance drive: a new brushless servo" , Motorcon Proceedings 147-160, 1985.
[3].   W. F. Ray, R. M. Davis, "Inverter drive for doubly-salient reluctance motor: its fundamental behaviour, linear analysis and cost implications", Proc. IEE, Pt. B, Elec. Power Application, vol.2, pp-185-193, 1979.
[4].   Fulton N. N., and Stephenson J. M., "A review of switched reluctance machine design", International Conference on Electrical Machines, 1988.
[5].   W. F. Ray, P. J. Lawrenson, R. M. Davis, J. M. Stephenson, N. N. Fulton and Roy J. Blake, "High-performance Switched Reluctance Brushless Drives", IEEE Transaction on Industry Applications, Vol. IA-22, No.4, July/August 1986, pp 722-730.
[6].   T J E Miller, "Converter Volt-Ampere requirements of the Switched Reluctance Motor Drive", IEEE Transactions on Industry Applications, Vol. IA-21, Sept/October, 1985, pp 1136-1134.
[7].   R. M. Davis, C. Eng, W. F. Ray and R. J. Blake, "Inverter drive for switched reluctance motor: circuits and component ratings", IEE Proceedings, Pt. B, vol. 128, pp 126-136, March 1981.

[8].   Bose B.K., Miller T.J.E., Szczesny PM, and Bicknell W.H., "Microcomputer control of Switched Reluctance motor", IEEE Transactions on Industry Application, Vol. IA-22, 1986, pp 708-715.
[9].   Miller T. J. E, Bower P. G., Becerra R, and Ehsani M, "Four quadrant brushless reluctance motor drive", IEE Conference on Power Electronics and Variable Speed Drives, London, 1988.
[10].   Miller T. J. E.,"Switched Reluctance Motors and Their Control", Magna Physics Publishing And Clarendon Press Oxford 1993.
[11].   El-Khazendar M. A. and Stephenson J. M.,"Analysis and optimisation of the 2-phase self-starting switched reluctance motor", ICEM, Munich, Sept. 8-10, 1031-1034.
[12].   H. A. Toliyat, Longya Xu and Thomas A. Lipo, "A five-phase reluctance motor with high specific torque", IEEE Transaction on Industry Applications, Vol. 28, No. 3, May/Juner, 1992, pp 659-667. 13.J. C. Moreiara and T. A. Lipo, "Simulation of a Four Phase Switched Reluctance Motor Including the Effect of Mutual Coupling," Electric Machines and Power Systems, vol. 16, pp. 281-299, 1989.
[13].   H. H. Moghbelli, G. E. Adams, and R. G. Hoft, "Prediction of the Instantaneous and Steady State Torque of the Switched Reluctance Motor Using the Finite Element Method (FEM)," IAS, pp. 59-70,1988.
[14].   D. S. Schramm, B. W. Williams, and T. C. Green, "Torque Ripple Reduction of Switched Reluctance Motors by Phase Current Optimal Profiling," PESC, pp. 857-860, 1992.
[15].   I. Husain and M. Ehsani, "Torque Ripple minimization in Switched Reluctance Motor Drives by PWM Current Control," IEEE Transactions on Power Electronics, vol. 11, no.1, pp. 83-88,1996.
[16].   M. Ilic-Spong, T. J. E. Miller, S. R. Macminn, and J. S. Thorp, "Instantaneous Torque Control of Electric Motor Drives," IEEE Transactions on Power Electronics, vol. 2, no.1, pp. 55-61,1987.
[17].   R. S. Wallace and D. G. Taylor, "A Balanced Commutator for Switched Reluctance Motors to Reduce Torque Ripple," IEEE Transactions on Power Electronics, vol. 7, no.4, pp. 617- 626,1992.
[18].   C. H. Kim and I. J. Ha, "A New Approach to Feedback-Linearizing Control of Variable Reluctance Motors for Direct-Drive Applications," IEEE Transactions on Control Systems, vol. 4, no. 4, pp. 348-362, 1996.
[19].   P. Pillay, Y. Liu, W. Cai, and T. Sebastian, " Multiphase operation of Switched Reluctance Motor Drives," IEEE Industry Applications Society Annual Meeting, Conference Record, pp. 310-317, 1997.
[20].   J. Faiz, B. Ganji, C.E. Carstensen, K.A. Kasper, R.W. De Doncker, "Temperature rise analysis of switched reluctance motors due to electromagnetic losses", IEEE Trans. on Magnetics, Vol. 45, No. 7, pp. 2927-2934, 2009.
[21].   H. Yahia, N. Liouane, R. Dhifaoui, "Multi-objective differential evolution-based performance optimization for switched reluctance motor drives", Turkish Journal of Electrical Engineering and Computer Sciences, Vol. 21, pp. 1061-1076, 2013.
[22].   J. Faiz, S. Pakdelian, "Diagnosis of static eccentricity in switched reluctance motors based on mutually induced voltages", IEEE Trans. on Magnetics, Vol. 44, No. 8, pp. 2029-2034, 2008.
[23].   J. Faiz, J. Raddadi, J.W. Finch, "Spice based dynamic analysis of a switched reluctance motor with multiple teeth per stator pole", IEEE Trans. on Magnetics, Vol. 38, No. 4, pp.1780-1788, 2002.
[24].   J. Faiz, J.W. Finch, "Aspects of design optimization for switched reluctance motors", IEEE Trans. on Energy Conversion, Vol. 8, pp. 704-713, 1993.
[25].   R.C. Kavanagh, J.M.D. Murphy, M.G. Egan, "Torque ripple minimization in switched reluctance drives using self-learning techniques", Proceeding of the IEEE/ IECI, pp. 289-294, 1991.
[26].   D.S. Schramm, B.W. Williams, T.C. Green, "Torque ripple reduction of switched reluctance motors by phase current optimal profiling", Proceeding of the IEEE/PES, pp. 857-860, 1992.
[27].   J.C. Moreira "Torque ripple minimization in switched reluctance motors via bi-cubic spline interpolation", Proceeding of the IEEE/PES, pp.851-856, 1992.
[28].   I. Husain, M. Ehsani, "Torque ripple minimization in switched reluctance motor drives by PWM current control", IEEE Trans. on Power Electronics, Vol. 11, No. 1, pp. 83-88, 1996.
[29].   N.C. Sahoo, S.K. Panda, P.K. Dash, "A current modulation scheme for direct torque control of switched reluctance motor using fuzzy-logic", Mechatronics, Vol.10, No. 3, pp. 353-370, 2000.
[30].   L.O.A.P. Henriques, L.G.B.Rolim, W.I. Suemitsu, P.J.C. Branco, J.A. Dente, "Torque ripple minimization in a switched reluctance drive by neuro - fuzzy compensation", IEEE Trans. on Power Electronics, Vol. 36, No. 5, 2000.
[31].   L. Kalaivani, N. S. Marimuthu, P. Subburaj, "Intelligent control for torque-ripple minimization in switched reluctance motor", Proceeding of the IEEE/ICEES, pp. 182-186, Newport Beach, CA, 2011.
[32].   N. C. Sahoo, J. X. Xu, S.K. Panda, "Low torque ripple control of switched reluctance motors using iterative learning," IEEE Trans. on Energy Conversion, Vol. 16, No. 4, pp. 318-326, 2001.
[33].   R. Mitra, W. Uddin, Y. Sozer, I. Husain, "Torque ripple minimization of switched reluctance motors using speed signal based phase current profiling", Proceeding of the IEEE/Energytech, Cleveland, OH , pp. 1-5, 2013.
[34].   I. Agirman, A. M. Stankovic, G.Tadmor, H. Lev-Ari, "Adaptive torque-ripple minimization in switched reluctance motors", IEEE Trans. on Power Electronics, Vol. 48, No. 3, pp. 664-672, 2001.
[35].   J.M. Stephenson, A. Hughes, R. Mann, "Torque ripple Minimization in a switched reluctance motor by optimum harmonic current injection", IEE Proc. Elect. Power Appl., Vol. 148, No. 4, 2001.
[36].   J. M. Stephenson, A. Hughes, R. Mann , "Online torque-ripple minimization in a switched reluctance motor over a wide speed range," IEE Proc. Electro. Power. Appl., Vol. 149, No. 4, 2002.
[37].   H. Tahresima, M. Kazemsaleh, M. Tahersima, N. Hamedi, "Optimization of speed control algorithm to achieve minimum torque ripple for a switched reluctance motor drive via GA", Proceeding of the IEEE/PESA, pp. 1-7, Hong Kong, 2011.
[38].   N. Inanc, V. Ozbulur, "Torque ripple minimization of a switched reluctance motor by using continuous sliding mode control technique", Electric Power System Research, Vol. 66, pp. 241-251, 2003.
[39].   N.T. Shaked, R. Rabinovici, "New procedures for minimizing the torque ripple in switched reluctance motors by optimizing the phase-current profile", IEEE Trans. on Magnetics, Vol. 41, No. 3, 2005.
[40].   R. Gobbi, K. Ramar, "Optimization techniques for a hysteresis current controller to minimize torque ripple in switched reluctance motors", IET Elect. Power Appl., Vol. 3, No. 5, pp. 453– 460, 2009.
[41].   C. Moron, A. Garcia, E. Tremps, J.A. Somolinos, "Torque control of switched reluctance motors", IEEE Trans. on Magnetics, Vol. 48, No. 4, pp. 1661-1664, 2012.
[42].   C. Mademlis, I. Kioskeridis, "Performance optimization in switched reluctance motor drives with online commutation angle control", IEEE Trans on Energy Conversion, Vol. 18, No. 3, 2003.

[43]. I. Kioskeridis and C. Mademlis, "Maximum efficiency in single - pulse controlled switched reluctance motor drives", IEEE Trans. on Energy Conversion, Vol. 20, No. 4, 2005.

[44]. J. Deskur, T. Pajchrowski and K. Zawirski, "Optimal control of current commutation of high speed SRM drive," IEEE International Conference on Power Electronics and Motion Control, pp. 1204 – 1208, 2008.

[45]. Ch. Lin, B. Fahami, "Optimization of commutation angles in SRM drives using FRM", IEEE international conference on transportation electrification, pp. 1-6, 2012.

[46]. E .F. I. Raj and V. Kamaraj, "Neural network based control for switched reluctance motor drive", Proceeding of the IEEE/ICETCCN, pp. 678-682, Tirunelveli, 2013.

[47]. D.H. Lee, J. Liang, Z. G. Lee, J. W. Ahn, "A simple nonlinear logical torque sharing function for low-torque ripple SR drive", IEEE Trans. on Industrial Electronics, Vol. 56, No. 8, pp. 3021-3028, 2009.

[48]. X.D. Xue, K.W. E. Cheng, S.L. Ho, "Optimization and evaluation of torque-sharing functions for torque ripple minimization in switched reluctance motor drives",IEEE Trans. on Power Electronics, Vol. 24, No. 9, 2009.

[49]. S.Y. Ahn, J.W. Ahn, D.H. Lee, "A novel torque controller design for high speed SRM using negative torque compensator", Proceeding of the IEEE/ICPE-ECCE, pp. 937-944, Jeju, South Korea, 2011.

[50]. V.P. Vujicic, "Minimization of torque ripple and copper losses in switched reluctance drive", IEEE Trans. on Power Electronics, Vol. 27, No. 1, pp. 388-399, 2012.

[51]. J. Faiz, F. Tahvilipour, Gh. Shahgholian, "Performance improvement of a switched reluctance motor", PIERS, Kuala Lumpur, Malaysia, pp.728-732, 2012.

[52]. J. Faiz, B. Rezaeealam, P. Pillay, "Adaptive performance improvement of switched reluctance motor with two-phase excitation", European Trans. on Electrical Power, Vol. 16, pp. 1-13, 2006.

[53]. Z. Lin, D.S. Reay, B. W. Williams and X. He, "Torque ripple reduction in switched reluctance motor drives using b-spline neural networks", IEEE Trans. on Industrial Applications, Vol. 42, No. 6, 2006.

[54]. Y. Cai, C. Gao, "Torque ripple minimization in SRM based on BP neural network", Proceeding of the IEEE/ICIEA, pp. 1198-1202, Harbin, P.R. China, 2007.

[55]. M. Rodrigues, P.J. Costa Branco, W. Suemitsu, "Fuzzy-logic torque ripple reduction by turn-off angle compensation for switched reluctance motors", IEEE Trans. on Industrial Electronics, Vol. 48, No. 3, pp. 711-715, 2001.

[56]. M. Divandari, R. Brazamini, A. Dadpour, M. Jazaeri, "A novel dynamic observer and torque ripple minimization via fuzzy-logic for SRM drives", Proceeding of the IEEE/ISlE, Seoul, South Korea, 2009.

[57]. C.L. Tseng, S.Y. Wang, Sh.Ch. Chien, Ch.Y. Chang, "Development of a self-tuning TSK- fuzzy speed control strategy for switched reluctance motor", IEEE Trans. on Power Electronics, Vol. 27, No. 4, pp. 2141-2152, 2012.

[58]. N. Tankachan and S. V. Reeba, "Tuned fuzzy-logic control of switched reluctance motor drives", Proceedings of the ICTITC, Vol. 150, pp. 655- 668, 2013.

[59]. A. Guettaf, F. Benchabame, M. Bahri, O. Bennis, "Torque ripple minimization in switched reluctance motor using the fuzzy-logic control technique", International Journal of System Assurance Engineering and Management, pp. 679-485, 2014.

[60]. J. Faiz, Gh. Shahgholian, H. Ghazizadeh, "Analysis of dynamic behavior of switched reluctance motor-design parameters effects", Proceeding of the IEEE/MELCON, pp.532-537, Valletta, Malta, 2010.

[61]. K. Russa, I. Husain, M.E. Elbuluk, "Torque-ripple minimization in switched reluctance machines over a wide speed range", IEEE Trans. on Industrial Application, Vol. 34, No. 5, pp. 1105-1112, 1998.

[62]. K. Russa, I. Husain, M. E. Elbuluk, "A self-tuning controller for switched reluctance motors", IEEE Trans. on Power Electronics, Vol. 15, No. 3, pp. 545-552, 2000.

[63]. I. Husain, "Minimization of torque ripple in SRM drives", IEEE Trans. on Industrial Electronics, Vol. 49, No. 1, pp. 28-39, 2002.

[64]. K.F. Wong, K.W.E. Cheng, S.L. Ho, "On-line instantaneous torque control of a switched reluctance motor based on co-energy control", IET Electric Power Applications, Vol. 3, No. 4, pp. 257–264, 2009.

[65]. S.K. Sahoo, S. Dasgupta, S.K. Panda, J.X. Xu, "A Lyapunov function- based robust direct torque controller for a switched reluctance motor drive system", IEEE Trans. on Power Electronics, Vol. 27, No. 2, pp. 555-564, 2012.

[66]. Sh. Sau, R. Vandana , B.G. Fernandes, "A new direct torque control method for switched reluctance motor with high torque/ampere", Proceeding of the IEEE/IES, pp. 2518-2523, 2013.

[67]. C. Ma, L. Qu, Z. Tang, "Torque ripple reduction for mutually coupled switched reluctance motor by bipolar excitations", Proceeding of the IEEE/ICEMD, pp. 1211-1217, 2013.

[68]. Y.K. Choi, H.S. Yoon, C.S. Koh, "Pole-shape optimization of a switched - reluctance motor for torque ripple reduction", IEEE Trans. on Magnetics, Vol. 43, No. 4, 2007.

[69]. D.H. Lee, T.H. Pham, J.W. Ahn, "Design and operation characteristics of four-two pole high-speed SRM for torque ripple reduction", IEEE Trans. on Industrial Electronics, Vol. 60, No. 9, 2013.

[70]. D.H. Lee, J.W. Ahn, "A novel four-level converter and instantaneous switching angle detector for high speed SRM drive", IEEE Trans. on Power Electronics, Vol. 22, No. 5, 2007.

[71]. A. Deriszadeh, E. Adib, H. Farzanehfard, S.M. Saghaian-Nejad, "New converter for switched reluctance motor drive with wide speed range operation", Proceeding of the IEEE/PEDSTTC, pp. 473- 477, 2011.

[72]. E. Daryabeigi, A. Emanian, "Torque ripple reduction of switched reluctance motor (SRM) drives, with emotional controller (BELBIC)", Proceeding of the IEEE/APECE, pp. 1528-1535, 2012.

[73]. M.J. Navardi, B. Babaghorbani, A. Ketabi, "Efficiency improvement and torque ripple minimization of SRM using FEM and seeker optimization algorithm ", Energy Conversion and Management, Vol. 78 , pp. 237–244, 2014.

[74]. L. Kalaivani , P. Subburaj, M. Willjuice , Iruthayarajan, "Speed control of SRM with torque ripple reduction using non-dominated sorting genetic algorithm (NSGA-II)", Electrical Power Energy Systems, Vol. 53, pp. 69-77, 2013.

[75]. D. Susitra , S. Paramasivam , " Rotor Position Eastimation for a Switched Reluctance Machine from Phase Flux Linkage", IOSR Journal of Electrical and Electronics Engineering (IOSR-JEEE) ISSN: 2278-1676 Volume 3, Issue 2 (Nov. - Dec. 2012), PP 07-14 .

[76]. R. A. Gupta, S.K.Bishnoi, "Sensorless Control of Switched Reluctance Motor Drive with Fuzzy Logic Based Rotor Position Estimation", ©2010 International Journal of Computer Applications (0975 - 8887) Volume 1 – No. 22 , pp. 72-79.

[77]. Maged N. F. Nashed, Samia M. Mahmoud , Mohsen Z. El-Sherif , and Emad S. Abdel-Aliem, " Optimum Change of Switching Angles on Switched Reluctance Motor Performance", International Journal of Current Engineering and Technology E-ISSN 2277 – 4106, P-ISSN 2347 - 5161 ©2014, pp.1052-1057.

[78]. Krzysztof Bieńkowski, Jan Szczypior, Bogdan Bucki, Adam Biernat, Adam Rogalski, "Influence of Geometrical Parameters of Switched Reluctance Motor on Electromagnetic Torque ",See discussions, stats, and author profiles for this publication at: https://www.researchgate.net/publication/228897332, 2004.

[79]. A. Bentounsi, "Optimized geometrical parameters of a SRM by numerical-analytical approach" See discussions, stats, and author profiles for this publication at: https://www.researchgate.net/publication/282026473, 2016.

[80]. A. Fleury, R. J. Dias, W. R. H. Araújo,A. W. F. V. Silveira, D. A. Andrade, G. C. Ribeiro, "Effects of the Mutual inductances on the Switched Reluctance Machines", International Conference on Renewable Energies and Power Quality (ICREPQ'12) Santiago de Compostela (Spain) , 2012, RE&PQJ, Vol.1, pp.1311-1316.

[81]. Zhangjun Tang, Pragasen Pillay, Avoki M. Omekanda,Chen Li, Cetin Cetinkaya, "Effects of Material Properties on Switched Reluctance Motor Vibration Determination", IEEE, 2003.

[82]. Senad Smaka, Mirsad Cosovic, Semsudin Masic," The Effects of Magnetic Circuit Geometry on Torque Generation of 8/14 Switched Reluctance Machine".

[83]. Balaji Mahadevan, "Sensitivity Analysis of Geometrical Parameters of a Switched Reluctance Motor with Modified Pole Shapes", Article in Journal of Electrical Engineering and Technology · January 2014,DOI: 10.5370/JEET.2014.9.1.136, PP. 136-142.

Deepa Bajpai'Brief History of Switched Reluctance Motor " IOSR Journal of Electrical and Electronics Engineering (IOSR-JEEE) 13.1 (2018): 01-25.